

Multi-Laser Scanning Confocal Fluorescent Endoscopy Scheme for Subcellular Imaging

Xiaomin Zheng^{1, #}, Xiang Li^{1, #}, Qiao Lin²,
Jiajie Chen^{1, *}, Yueqing Gu², and Yonghong Shao^{1, *}

(Invited)

Abstract—Fluorescence confocal laser scanning endomicroscopy is a novel tool combining confocal microscopy and endoscopy for in-vivo subcellular structure imaging with comparable resolution as the traditional microscope. In this paper, we propose a three-channel fluorescence confocal microscopy system based on fiber bundle and two excitation laser lines of 488 nm and 650 nm. Three fluorescent photomultiplier detecting channels of red, green and blue can record multi-color fluorescence signals from single sample site simultaneously. And its ability for in-vivo multi-channel fluorescence detection at subcellular level is verified. Moreover, the system has achieved an effective field of view of 154 μm in diameter with high resolution. With its multi-laser scanning, multi-channel detection, flexible probing, and in-vivo imaging abilities it will become a powerful tool in bio-chemical research and diagnostics, such as the investigation of the transport mechanism of nano-drugs in small animals.

1. INTRODUCTION

With the development and demand of clinical diagnosis, the emergence of confocal endoscopic imaging technology that combines laser scanning confocal fluorescence imaging and endoscopic technology has become a new research hotspot [1, 2], and it can realize real-time nondestructive imaging of living bodies at cell level. The confocal microscopy has developed rapidly since it was proposed by Marvin Minsky in 1957. The system greatly improves the microscopic signal-to-noise ratio and axial resolution by adopting point light source and conjugated pinhole [3, 4]. With that configuration, most of the out-of-plane signals are blocked, and majority of the signals from the focal plane can be collected by a single pixel detector. The size of the pinhole determines the axial resolution, and the optimal detection aperture size is 60% ~ 80% of the diffraction spot [5]. In 1993, Gmitro and Aziz first proposed the use of fiber bundle for the transmission of the specimen images at the focal plane, and in their design, each single fiber in the fiber bundle acts as a point light source and a confocal pinhole at the same time, which established the typical principle of fiber-based laser scanning confocal micro-endoscopy [6]. Thereafter, various performance improvement methods have been developed. For example, Ye et al. studied microscopic endoscopes based on spectrally-encoded scanning. They used a single fiber and a transmission micro-grating to disperse the white light to achieve one-dimensional spectrally encoded scanning, and the system can probe into small organs such as breast and pancreas [7]. In addition, Li et al. developed a resonant fiber-optic piezoelectric scanner for spiral scanning via four piezoelectric elements arranged in a square tube [8]. Moreover, Liu et al. adopted two low numerical aperture

Received 22 September 2020, Accepted 16 November 2020, Scheduled 25 November 2020

* Corresponding author: Jiajie Chen (cjj@szu.edu.cn), Yonghong Shao (shaoyh@szu.edu.cn).

¹ Key Laboratory of Optoelectronic Devices and Systems of Ministry of Education and Guangdong Province, College of Physics and Optoelectronics Engineering, Shenzhen University, Shenzhen 518060, China. ² State Key Laboratory of Natural Medicines, Department of Biomedical Engineering, School of Engineering, China Pharmaceutical University, Nanjing 210009, China. # These authors contributed equal to the article.

objectives in the confocal microscope endoscope, which results in deeper optical section depth and higher axial resolution [9]. Therefore, the imaging speed and imaging quality of the confocal endoscope can be improved by adopting efficient scanning method, miniature objective lens, and specifically designed high precise optical components.

In this paper, we propose a multi-color laser scanning confocal fluorescence endoscopic system. The full width at half maximum (FWHM) of the imaging system's point spread function (PSF) is $0.51 \mu\text{m}$. The diameter of field of view of the system is $154 \mu\text{m}$ with the imaging speed of 2 fps. A three-channel imaging system was utilized to image U87 cells and mouse heart tissue sections stained with three different fluorescent dyes. The results have not only verified the multi-color laser scanning ability of the confocal fluorescence endoscope but also proved its ability of subcellular imaging. Moreover, the in-vivo subcellular imaging ability has also been verified on multi-fluorescence-labeled mice.

2. METHODS OF AND RESULTS

Figure 1 is the schematic diagram of the fiber bundle based three-channel confocal endoscope. The light source of the system is two semiconductor continuous lasers with the wavelengths of 488 nm and 650 nm (MBL-SF-488-70 mW, CNI, China; MRL-III-650L-200 mW, CNI, China). The output lights of two lasers are combined through dichroic mirrors (DM1 and DM2). The two-color coaxial beams are reflected together by the dichroic mirror (DM2), then enter the spatial filtering system consisting of objective lens 1 (Obj1), pinhole ($40 \mu\text{m}$, Opm, China), and objective lens 2 (Obj2). The spatial filtering system blocks out-of-focusing fluorescence signal and regulates the excitation light. Subsequently, the beam is reflected by a two-dimensional scanning galvanometer (GM), enters into a 4f optical system consisting of lens groups of L1 and L2 [10], and then is coupled into the optical fiber bundle which consists of about 30,000 fibers (each fiber's core diameter is $1.1 \mu\text{m}$) via objective lens 3 (Obj3). Each fiber in the fiber bundle serves as a point light source and confocal pinhole for laser excitation and fluorescence transmission. When the front focal plane of the Obj3 is completely coincident with the left end of the fiber bundle, the light beam in the optical fiber core is effectively transmitted, and a clear

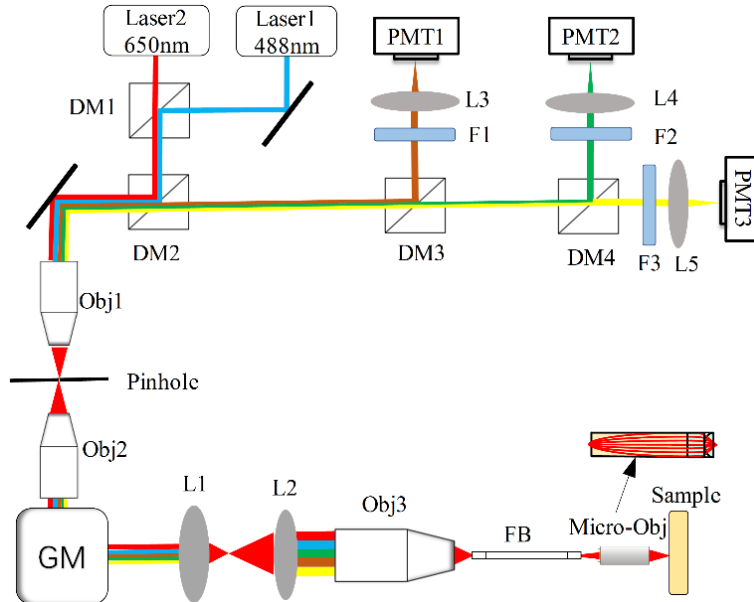


Figure 1. Principle of a three-channel confocal endoscope system. DM: Dichroic Mirrors (DM1, T525lpxr; DM2, ZET405/488/561/647; DM3: T560lpxr; DM4: T647lpxr; Chroma Inc.); Obj: Objective Lens, Obj1, 2 ($10\times/0.25$, Olympus, Japan), Obj 3 ($20\times/0.5$, Olympus, Japan); GM: 2D Galvanometric Scanning System; L: Lens; FB: Fiber bundle (FIGH-30-850N, Fujikura, Japan); Micro-Obj: Micro-Objective; F: Band Pass Filter; PMT: Photomultiplier.

image is obtained [11]. A $4.65\times$ micro-objective ($NA = 0.8$; Diameter: 3 mm; Length: 7.5 mm; working distance: $80\ \mu\text{m}$) which consists of a GRIN lens (gradient refractive index lens) and a micro-lens is placed at the fiber bundle end. It focuses the excitation light beam onto the sample and also collects the fluorescence signal from the sample. Note that the pinhole is conjugated to the focal point of the Obj3 as well the micro-objective, so only the signal from the micro-objective focal point can be collected. Although each fiber in the fiber bundle is also functional as the “pinhole”, the pinhole between the Obj1 and Obj2 provides a narrower constraint to further block the crosstalk between different fibers.

For the signal detection part, a series of dichroic mirrors (DM2, 3, 4) with different reflection spectral bands separate different fluorescent signals into different channels, and the signals are detected by PMTs (7420-40, Hamamatsu, Japan) and transferred into electrical signal. Then it is transmitted to the data acquisition card (PCI 6110, National Instruments, United States), which also controls the scanning sequence of the galvanometer, thereby controlling the point scanning of the laser and the timing of the fluorescence signal. Three images of two-dimensional fluorescence signals are acquired simultaneously through the subsequent two-dimensional reconstruction. To access the imaging quality of the system, we image fluorescent beads with the size of $100\ \text{nm}$ in diameter (Ex/Em: $488\ \text{nm}/560\ \text{nm}$) to measure the system's PSF. As shown in the results of Figure 2, the normalized intensity curve along the yellow line through the center of the fluorescent bead image indicates that the FWHM of the PSF is $0.51\ \mu\text{m}$. By moving the fluorescent bead sample via high-precision translation stage (NanoMax 3-Axis Flexure Stage), we obtained the pixel size of the image ($0.15\ \mu\text{m}$) and the field of view in diameter ($154\ \mu\text{m}$). Note that there exists a honeycomb pattern in the image because of the intervals between fibers in the fiber bundle. Therefore, the actual imaging quality cannot reach the level of a confocal microscope [12]. Although there are several spatial filtering methods to eliminate the honeycomb pattern, they may lower the image contrast and signal level [13]. Therefore, in our scheme, in order to maintain a higher image contrast, we adopted the original image for the following experiments.

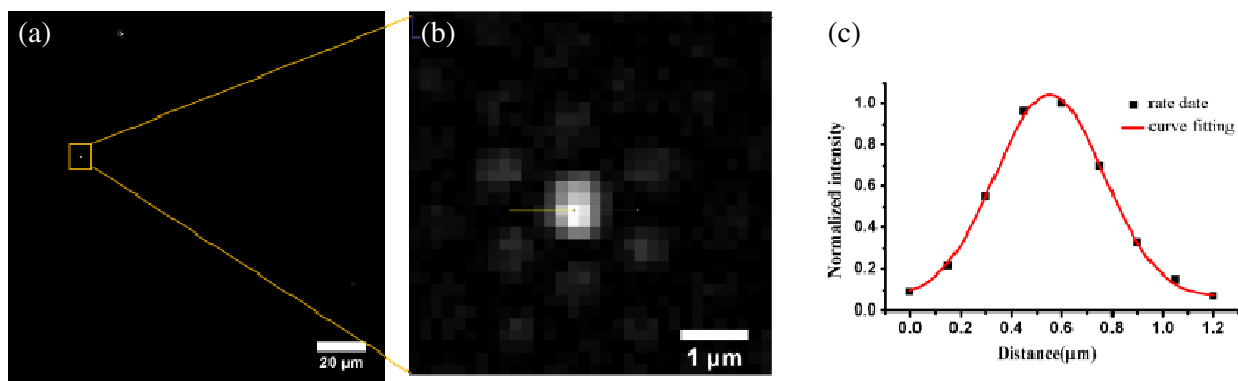


Figure 2. Schematic diagram of fluorescent bead imaging and full width at half maximum obtained by Gaussian fitting. (a) Image of multiple fluorescent beads in the whole field of view. (b) Zoom-in image of a single fluorescent bead. (c) The normalized intensity profile of the fluorescent bead along the yellow line.

To evaluate the performance of our endoscope system, three fluorescent dyes, FITC (Fluorescein Isothiocyanate), DiA (4-(4-(Dihexadecylamino) styryl)-N-methylpyridinium iodide), and R3 are selected, and their fluorescent spectra are shown in Figure 3. FITC is a widely used fluorescent dye for whole cell body staining [14]. The maximum absorption wavelength of FITC is within the range of $490\ \text{nm}$ to $495\ \text{nm}$, and the maximum emission wavelength is within the range of $520\ \text{nm}$ to $530\ \text{nm}$. As a lipophilic fluorescent dye, DIA is often used to label cell membranes or other hydrophobic tissues. The maximum absorption wavelength and emission wavelength of DiA are $491\ \text{nm}$ and $613\ \text{nm}$, respectively. Therefore, in our experiment, $488\ \text{nm}$ laser can excite the fluorescence of FITC and DiA simultaneously. In addition, R3 is a fluorescent reagent developed independently from our cooperative research laboratory [15]. It can produce strong fluorescence signal which is suitable for labeling peptides, proteins, nano drug carriers, etc. Its maximum absorption wavelength is $650\ \text{nm}$, and the maximum

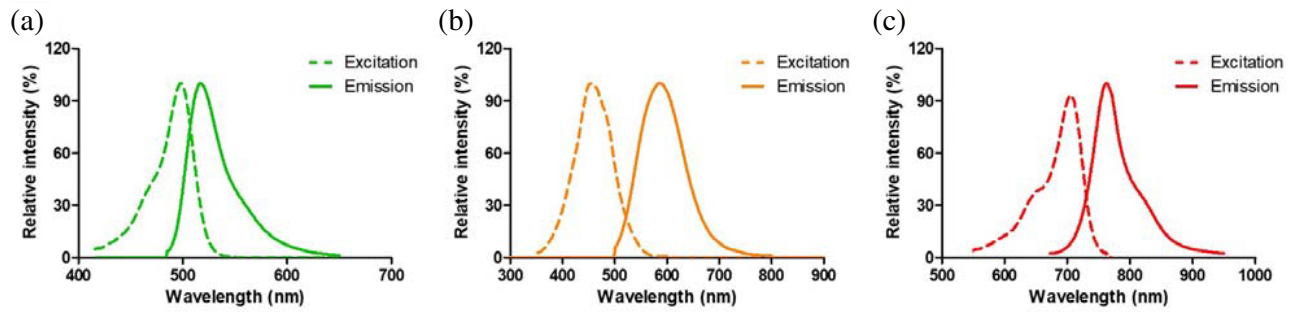


Figure 3. Dye spectral curve of excitation and emission. (a), (b), and (c) are the fluorescence spectra of the fluorescent dyes of FITC and DiA, and R3, respectively. The dotted line is the excitation spectrum, and the solid line is the emission spectrum.

emission wavelength is 730 nm. In our experiment, 650 nm laser is adopted for the excitation.

In the bio-sample imaging experiments, we imaged the myocardial tissue of mice stained with three fluorescent dyes (FITC, DiA, and R3). For the bio-sample preparation, we euthanized a healthy adult ICR mouse, then we removed the heart and cleaned it in 0.9% NaCl solution. The entire heart tissue was embedded with an appropriate amount of OTC agent and quickly frozen in a liquid nitrogen tank. Then we performed tissue sections on a frozen microtome. After that, they were incubated with 5 μ M mixed fluorescent dyes (FITC, DiA, and R3) in the dark for 30 minutes and washed carefully with PBS solution. Three images obtained simultaneously in real time by the system are shown in Figure 4. A structure and morphology of myocardial tissue can be clearly observed. It also shows that the image shows high definition and contrast.

In addition, we also tested its ability for cell imaging. We seeded and cultured the U87 cells in the logarithmic growth phase on sterile cell slides at 37°C and in 5% CO₂. When the cell fusion percentage reached 70–80%, the cells were fixed with 4% paraformaldehyde for 20 minutes. The cells were incubated

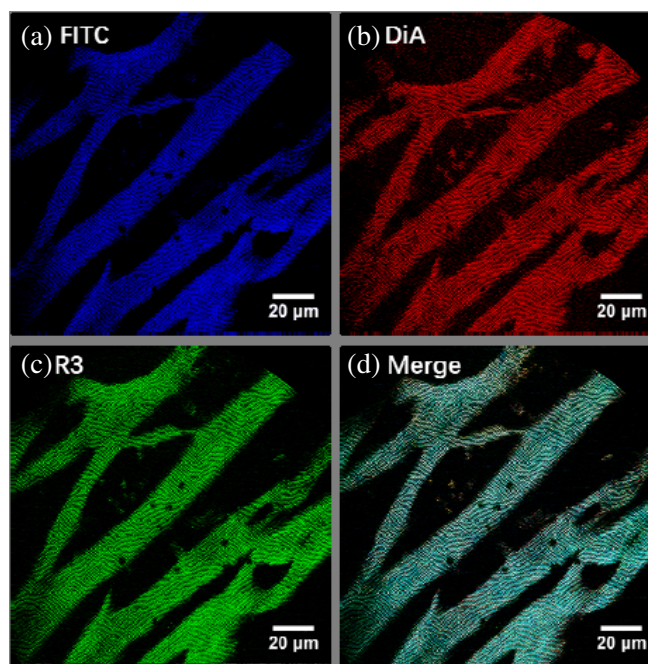


Figure 4. Image of myocardial tissue stained with three dyes. (a)–(c) are myocardial tissue images stained with fluorescent dyes FITC, DiA, and R3, respectively. (d) Merged image.

in a 37°C incubator with 5 μM mixed fluorescent dyes (FITC, DiA, and R3) in the dark for 30 minutes. FITC and R3 are cell-free dyes that can stain the entire cell while DiA is a cell membrane fluorescent dye. The different structures of cells in three channels are obtained. As shown in Figure 5, one can clearly

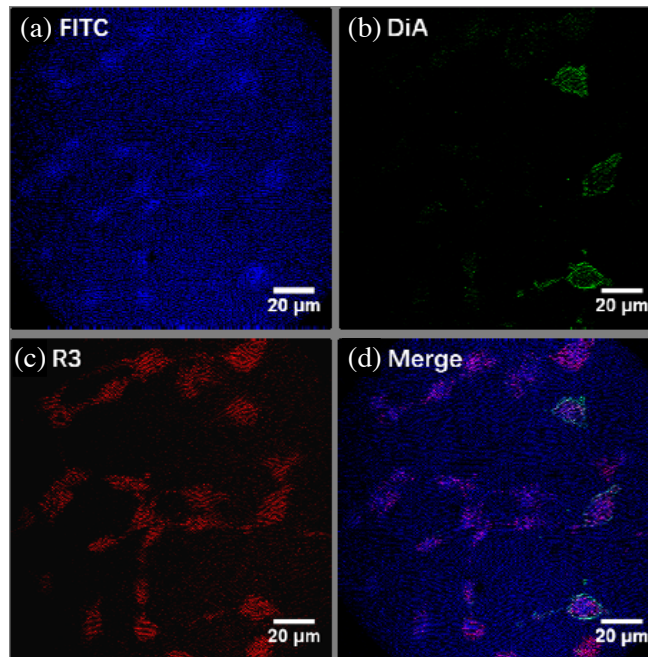


Figure 5. Image of the U87 cells stained with three dyes. (a), (b), and (c) are the U87 cells images stained with fluorescent dyes FITC, DiA, and R3, respectively. (d) Merged image.

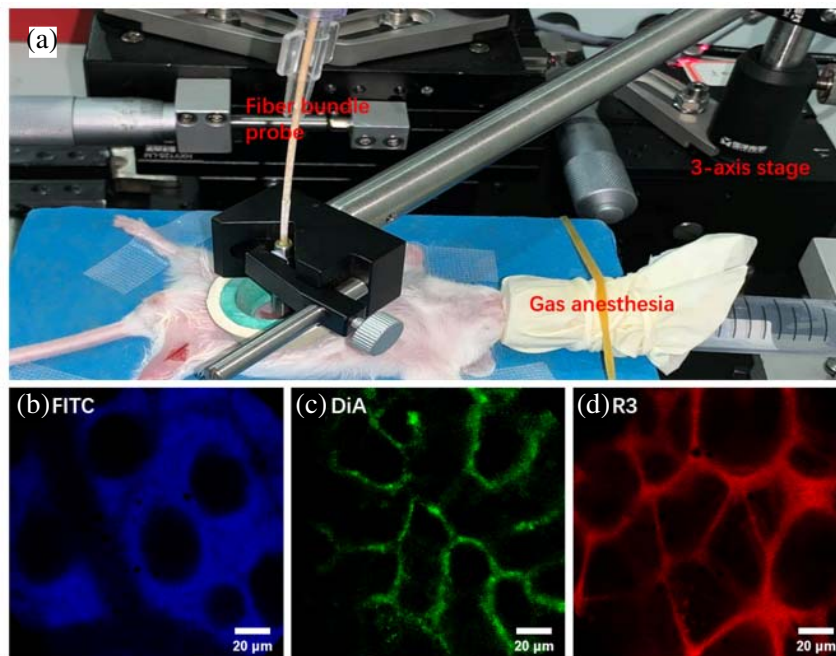


Figure 6. In-vivo endoscopic imaging of mice tissues. (a) is the operation stage and optical setup; (b)–(d) is the fluorescence images of intestine, kidney and adipose of living mice after intravenous injection of FITC, DIA and R3 respectively.

observe the image of cell structures of different staining fluorescence and distinguish the cell membranes and cytoplasm in the merged image. The results indicate that the proposed confocal endoscope system presents clear multi-color subcellular imaging ability with high accuracy.

Moreover, we also tested the in-vivo imaging ability using the fluorescence-labeled mice. For the test preparation, ICR mice were anesthetized with isoflurane and fixed on the operating table. FITC, DIA, and R3 solutions prepared with normal saline were injected into the tail vein of mice with the dose of 1.5 mg/kg, and the injection volume was 200 μ L. During the imaging experiments, the abdominal organs of mice were exposed after skin shaving. As shown in Figure 6, due to the differences of the diffusion process of the three dyes, FITC, DIA, and R3 were detected in intestine, kidney, and adipose, respectively. Therefore, by adopting the dual-wavelength three-channel endoscopic imaging in living mouse tissues, one can see that the crypt and blood capillaries can be clearly distinguished in the intestine, and the structure of renal tubules is clear and complete with high resolution. The adipose tissue clearly shows the intercellular space between adipocytes after R3 staining. Therefore, the capability for in-vivo endoscopic microscopic imaging of fluorescence-labeled tissues is verified, which has made it a powerful tool for monitoring the transportation mechanism of nano-drugs in small animals.

3. SUMMARY AND DISCUSSION

In this paper, a multi-color fiber bundle based confocal fluorescence microscopic endoscope system is developed. The system contains three fluorescence channels, and it can simultaneously image the cells and tissues stained with three kinds of dyes. The ability of the system to discriminate the structural information of tissue samples is also verified. With further development, the system can be used to in-vivo monitor the dynamic process of physiological activities of various fluorescent labeling substances in the living cells of small animals.

Multi-colored confocal endoscope enables the in-vivo imaging of cellular tissue levels with more structural information. However, there is still much room for further improvement. First, the detection depth of the endoscope limits our scope of observation at the tissue surface. Note that the near-infrared confocal endoscope technology can image tissue cells to a depth of 300 μ m [16]. However, this is currently unattainable for multicolor confocal endoscopes. Further research will focus on the combination of near-infrared technology and multicolor confocal endoscope, so that one can conduct multicolor confocal endoscopes with deeper imaging depth, which will make a great contribution to the early lesions diagnosis. Second, the miniaturization of confocal endoscope probes has been realized, and various kinds of probes are developed, such as S series for surface imaging. These probes are also compatible with our multi-color confocal endoscope system, which make it more versatile in practical applications.

In summary, the proposed three-channel miniaturized confocal endoscope can perform in-vivo imaging on tissues and cells level with high diagnostic accuracy. The three-channel multi-fluorescence detection scheme has shown great advantages over the traditional single-channel probe mode. More multi-functional dyes are applicable to the imaging system. A variety of dyes with the properties of specific antibodies labeling, lower toxicity to the human body, or specific clinical function can be adopted [17]. Moreover, the flexible probing capability of the fiber bundle has also expanded the application of the imaging scheme to more complex imaging scenarios in various kinds of bio-samples. With further development, we believe that the system can be adopted in clinical use such as in-vivo tissue biopsy and early diagnosis of digestive tract pathological inspection.

ACKNOWLEDGMENT

This work was supported by the Project from the National Natural Science Foundation of China (61527827, 81727804, 61905145 and 61775148); National Key Research and Development Program of China (2017YFB0403804); Guangdong Natural Science Foundation and Province Project (2017B020210006); Shenzhen Science and Technology R&D and Innovation Foundation (JCYJ20180305124754860).

REFERENCES

1. Quinn, M. K., T. C. Bubi, M. C. Pierce, M. K. Kayembe, D. Ramogola-Masire, and R. Richards-Kortum, "High-resolution microendoscopy for the detection of cervical neoplasia in low-resource settings," *Plos One*, Vol. 7, No. 9, e44924, 2012.
2. Becker, V., S. von Delius, M. Bajbouj, A. Karagianni, R. M. Sclunid, and A. Meining, "Intravenous application of fluorescein for confocal laser scanning microscopy: Evaluation of contrast dynamics and image quality with increasing injection-to-imaging time," *Gastrointestinal Endoscopy*, Vol. 68, No. 2, 319–323, 2008.
3. Jabbour, J. M., M. A. Saldua, J. N. Bixler, and K. C. Maitland, "Confocal endomicroscopy: Instrumentation and medical applications," *Annals of Biomedical Engineering*, Vol. 40, No. 2, 378–397, 2008.
4. Veronika, N., K. Alexandr, T. Pavel, and S. Sarka, "Scanning probe microscopy as a tool for investigation of biomaterials," *Advance in Electrical and Electronic Engineering*, Vol. 10, No. 5, 350–354, 2012.
5. Sandison, D. R., D. W. Piston, R. M. Williams, and W. W. Webb, "Quantitative comparison of background rejection, signal-to-noise ratio, and resolution in confocal and full-field laser scanning microscopes," *Applied Optics*, Vol. 34, No. 19, 3576–3588, 1995.
6. Gmitro, A. F. and D. Aziz, "Confocal microscopy through a fiber-optic imaging bundle," *Optics Letters*, Vol. 18, No. 8, 565–567, 1993.
7. Ye, L. D., I. Rizvi, W. M. White, J. T. Motz, T. Hasan, B. E. Bouma, and G. J. Tearney, "Three-dimensional miniature endoscopy," *Nature*, Vol. 443, No. 7113, 765–765, 2006.
8. Li, Z., Z. Yang, and L. Fu, "Scanning properties of a resonant fiber-optic piezoelectric scanner," *Review of Scientific Instruments*, Vol. 82, No. 12, 123707, 2011.
9. Liu, J. T. C., M. J. Mandella, H. Ra, L. K. Wong, and T. D. Wang, "Miniature near-infrared dual-axes confocal microscope utilizing a two-dimensional microelectromechanical systems scanner," *Optics Letters*, Vol. 23, No. 3, 256–258, 2007.
10. David, S., O. Lubos, T. Jan, I. Tomas, and O. Jakub, "Biometric image recognition based on optical correlator," *Advance in Electrical and Electronic Engineering*, Vol. 15, No. 2, 343–351, 2017.
11. Wang, J., M. Yang, L. Yang, Y. Zhang, J. Yuan, Q. Liu, X. Hou, and L. Fu, "A confocal endoscope for cellular imaging," *Engineering*, Vol. 1, No. 3, 351–360, 2015.
12. Maitland, K. C., A. M. Gillenwater, M. D. Williams, A. K. El-Naggar, M. R. Descour, and R. R. Richards-Kortum, "In vivo imaging of oral neoplasia using a miniaturized fiber optic confocal reflectance microscope," *Oral Oncology*, Vol. 44, No. 11, 1059–1066, 2008.
13. Park, S. C., M. K. Park, and M. G. Kang, "Super-resolution image reconstruction: A technical overview," *IEEE Signal Processing Magazine*, Vol. 20, No. 3, 21–36, 2003.
14. Elahi, S. E., S. J. Miller, and T. D. Wang, "Targeted imaging of colorectal dysplasia in living mice with a confocal microendoscope," *Gastroenterology*, Vol. 140, No. 5, S763–S764, 2011.
15. Wang, J., H. Li, G. Tian, Y. Deng, Q. Liu, and L. Fu, "Near-infrared probe-based confocal microendoscope for deep-tissue imaging," *Biomedical Optics Express*, Vol. 9, No. 10, 5011–5025, 2018.
16. Ma, Y., Z. H. Wang, Y. X. Ma, Z. H. Han, M. Zhang, H. Y. Chen, and Y. Q. Gu, "A telomerase-responsive DNA icosahedron for precise delivery of platinum nanodrugs to cisplatin-resistant cancer," *Angew. Chem. Int. Ed. Engl.*, Vol. 57, No. 19, 5389–5393, 2018.
17. Foersch, S., R. Kiesslich, M. J. Waldner, P. Delaney, P. R. Galle, M. F. Neurath, and M. Goetz, "Molecular imaging of VEGF in gastrointestinal cancer in vivo using confocal laser endomicroscopy," *Gut*, Vol. 59, No. 8, 1046–1055, 2010.